Life-Cycle Management of Fatigue-Sensitive Structures Integrating Inspection Information

S. Mohamed Soliman, S.M.ASCE[1]; and Dan M. Frangopol, Dist.M.ASCE[2]

Abstract: Successful management of deteriorating structures requires the reliable prediction of damage occurrence as well as the time-dependent damage propagation under uncertainty. The reliability of the performance prediction process can be significantly improved by integrating information gained from inspection and monitoring actions. This integration leads to a more accurate prediction of the time-dependent damage level and, eventually, to a better supported decision-making process. In this paper, a probabilistic approach is proposed to find an optimum management plan for fatigue-sensitive structures by integrating the available information from inspection actions. The proposed approach utilizes a probabilistic time-dependent damage criterion, inspection cost, and failure cost to find the optimum inspection times under uncertainty. New information resulting from inspection actions performed during the lifetime of the structure is used to update the damage propagation parameters as well as the optimization procedure. This process results in an enhanced management plan which can provide managers the ability to make real-time decisions based on inspection results. The integration of this new information and its impact on the life-cycle management process are thoroughly investigated. In addition, a realistic fatigue critical detail is used to illustrate the proposed probabilistic approach. **DOI: 10.1061/(ASCE)IS.1943-555X.0000169.**

Author keywords: Fatigue; Inspection scheduling; Optimization; Bayesian updating; Crack growth; Life cycle.

Introduction

Fatigue cracking is an endangering effect on the safety of steel structures. The need to provide new approaches for effective fatigue life-cycle management (LCM) of such structures is growing. Effective LCM plans should provide information regarding fatigue critical locations, optimized inspections, monitoring, and repair times (Das 2000; Frangopol 2011). Effective inspection and monitoring actions are crucial aspects in the LCM framework. They provide the useful means to: (1) reduce uncertainties in the loading and resistance of the structure, (2) indicate the current condition of the structure, and (3) detect the possible damaged locations within the structure. Since the results of these actions allow for decision making, the inspection and monitoring times should be optimized to ensure that damage will be detected before causing a significant drop in the structural performance. For this reason, in recent years, the optimum planning for inspection and monitoring actions in a life-cycle context has gained higher importance (Enright and Frangopol 1999; Estes and Frangopol 2001; Onoufriou and Frangopol 2002; Neves et al. 2006a, b). On the other hand, the results of inspection and monitoring actions may not give a clear indication on the future propagation of a detected damage. Accordingly, maintenance and repair actions should be planned based on the inspection/monitoring outcomes along with the results of the prediction models under uncertainty (Zheng and Ellingwood 1998).

In the last few decades, research efforts have been made in the field of inspection/monitoring planning for steel and aluminum structures subjected to fatigue. The results have shown that optimum inspection/monitoring plans that fulfill the management goals can be achieved. Examples of these goals include minimizing the total life-cycle cost, maximizing the service life of the structure, and minimizing the damage detection delay (Cramer and Friis-Hansen 1994; Garbatov and Guedes Soares 2001; Chung et al. 2006; Kale and Haftka 2008; Kim and Frangopol 2011; Kwon and Frangopol 2011). Studies in this field can use the damage propagation profile, such as the crack growth profile based on linear elastic fracture mechanics (LEFM), as the performance measure or a probabilistic performance indicator, such as the time-variant reliability index and probability of failure, and the lifetime functions. These studies handled the scheduling process by providing inspection and repair schedules that optimize the management goals. For repair scheduling, an appropriate repair strategy is selected in the optimization procedure based on the predicted crack size at each inspection and the probability of damage detection (e.g., Madsen et al. 1991; Kwon and Frangopol 2011; Kim et al. 2013). Despite its effectiveness, this approach in repair scheduling does not allow the integration of new information collected through future inspection or monitoring actions into the existing management plans. In general, detecting a damage level that is significantly different from the predicted one would indicate that the prediction model may not be suitable for addressing the problem.

In an attempt to address this issue, other inspection and repair scheduling procedures were proposed. These procedures considered updating the structural performance indicators of the inspected location based on the inspection results. This can be performed by defining time-based safety margins and updating the time-variant probability of failure according to inspection outcomes. Madsen et al. (1987, 1991) proposed an approach which uses the LEFM to perform inspection and repair scheduling. Based on the inspection outcomes, the failure probabilities and probabilities of repair are

[1]Graduate Research Assistant, Dept. of Civil and Environmental Engineering, ATLSS Engineering Research Center, Lehigh Univ., Bethlehem, PA 18015-4729. E-mail: mos209@lehigh.edu

[2]Professor and the Fazlur R. Khan Endowed Chair of Structural Engineering and Architecture, Dept. of Civil and Environmental Engineering, ATLSS Engineering Research Center, Lehigh Univ., Bethlehem, PA 18015-4729 (corresponding author). E-mail: dan.frangopol@lehigh.edu

Note. This manuscript was submitted on June 21, 2012; approved on May 13, 2013; published online on May 15, 2013. Discussion period open until June 6, 2014; separate discussions must be submitted for individual papers. This paper is part of the ***Journal of Infrastructure Systems***, © ASCE, ISSN 1076-0342/04014001(13)/$25.00.

updated by conditioning them upon the inspection outcomes. Cramer and Bea (1991) used an *S-N* approach combined with formulae which relate to the crack size to the remaining service life of through thickness cracks in order to calculate the time-variant probability of failure for the detail being studied. Moan and Song (2000) proposed a reliability-based model that can find the reliability of a series of inspected and uninspected fatigue details. In their approach, the reliability of the system was updated based on the results of inspection of several components in the system. The discussed reliability-based inspection scheduling methods plan the inspection based on the predicted reliability profile and the target reliability index; i.e., an inspection is performed when the reliability index reaches the threshold value. If updating is performed, yielding an updated reliability profile, the next inspection is scheduled when the updated profile reaches the threshold. However, the updating process in this manner does not modify the model parameters based on the inspection outcomes and, therefore, the updated reliability profile may not be representative of the actual damage propagation. Therefore, the results of the updated inspection scheme may be questionable, especially considering the fact that the detected damage level, in most cases, will be different than the predicted one at the inspection time (Zheng and Ellingwood 1998).

An alternative approach is to use Bayesian updating of the damage propagation model parameters. In this approach, the information from inspection actions is used to represent the likelihood function, which can be combined with the prior knowledge of the model parameters to yield an updated posterior distribution of the model parameters. Next the performance prediction is performed using the posterior parameters to achieve more reliable results. This approach was investigated by Heredia-Zavoni and Montes-Iturrizaga (2004). They used the probability of detection in an updating procedure to predict the posterior distribution of the initial crack size at a certain point in time, and the measurement was used as the new data to update the probability density function of the initial crack size. However, inspection optimization and scheduling was not considered as a goal of the study. Perrin et al. (2007) used Bayesian techniques and Markov chain Monte Carlo (MCMC) for fatigue crack growth analysis based on data collected during experimental investigations. Their results showed the feasibility of updating the model parameters based on crack size measurements. Li et al. (2011) used Bayesian updating to study the effect of the sensor degradation on the estimation of the remaining useful life of structures. None of these performance updating studies was aimed to provide an optimal inspection schedule under uncertainty. Additionally, these studies do not directly support the decision making process since the management actions based on inspection outcomes are not provided. Thus, there still exists the need for integrated management plans that provide optimal intervention times and types while making use of the available inspection and monitoring information to improve the performance prediction process, and hence, better and effective decisions can be made.

In this paper, a life-cycle management framework for fatigue critical structures integrating inspection outcomes is proposed. A cost-based optimization approach is formulated to find the optimal inspection times while considering uncertainties associated with the damage propagation model and the damage detection technique. The optimization approach finds the optimal inspection time, which minimizes the life-cycle cost consisting of inspection and failure costs, for each of the considered inspection methods. Bayesian updating is used to find the posterior distributions of fatigue crack growth model parameters based on inspection results. The updated models are subsequently used to find the next inspection times based on the measured crack size. By analyzing the space

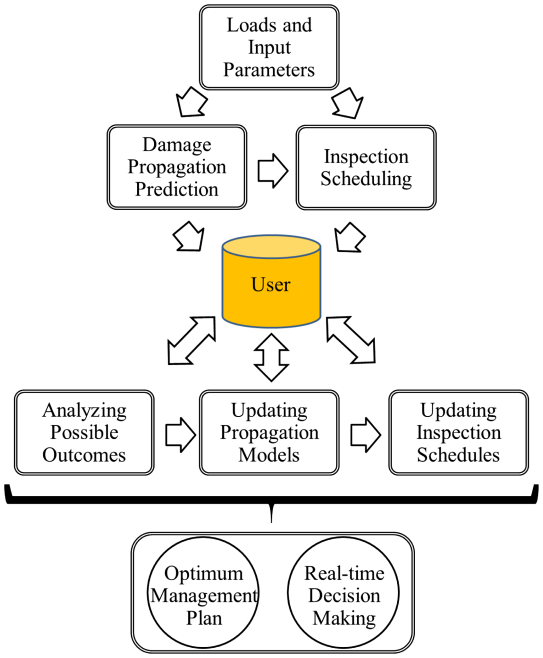

Fig. 1. Schematic for the proposed management framework

of possible inspection outcomes, effective inspection plans can be achieved and rational real-time decisions regarding future inspection and/or rehabilitation actions can be made. The proposed framework is shown in Fig. 1. Each of the modules in Fig. 1 will be discussed in detail in the following sections of this paper.

Fatigue Damage in Steel Structures (A Brief Review)

Fabrication of steel structures may result in the presence of initial cracks or crack-like conditions in multiple locations of the structure. The repetition of loads at these locations can lead to crack propagation, and eventually to failure (Fisher et al. 1998). The crack growth at a certain location depends on the loading conditions, material properties, initial crack size, and the geometry of the detail (Fisher 1984). Among the several available models for crack propagation, the Paris equation (Paris and Erdogan 1963) will be used herein to predict the time-variant crack size. This equation relates the ratio of the increment in crack size to the specific loading cycle and range of the stress intensity factor ΔK through

$$\frac{da}{dN} = C(\Delta K)^m \tag{1}$$

where a = crack size; N = number of cycles; and C and m = material parameters. The range of the stress intensity factor ΔK is expressed as

$$\Delta K = S_{re} \cdot G(a)\sqrt{\pi a} \tag{2}$$

where S_{re} = stress range and $G(a)$ = geometry function. Using Eqs. (1) and (2), the cumulative number of cycles required for a crack to grow from an initial size a_o to a size a_N is

$$N = \frac{1}{C \cdot S_{re}^m} \int_{a_o}^{a_N} \frac{da}{[G(a)\sqrt{\pi \cdot a}]^m} \tag{3}$$

The corresponding time associated with the crack growth from a size a_o to a_N can be calculated by considering the annual average number of cycles N_{avg} as

$$t = \frac{1}{N_{\text{avg}} \cdot C \cdot S_{re}^{m}} \cdot \int_{a_o}^{a_N} \frac{da}{[G(a)\sqrt{\pi \cdot a}]^m} \tag{4}$$

The expected service life of a detail can be calculated using Eq. (4) by considering the crack size a_N to be equal to the critical crack size. The calculated service life using this model will be subsequently used to find the optimum inspection times for the detail.

Nondestructive Fatigue Inspection of Steel Bridges

Fatigue critical structures such as steel bridges, offshore structures, and ships are inspected at regular or irregular time periods to spot any damage in the structure and apply the required maintenance actions. Recent research has shown that irregular inspection schedules are more cost-effective than regular inspection plans (Kwon and Frangopol 2011). These inspections are crucial to maintain the structural integrity. The probability of detection, which is defined as the probability of detecting an existing crack with a specific size using an inspection method (Chung et al. 2006), is generally used to represent the quality of the inspection method (Frangopol et al. 1997; Zheng and Ellingwood 1998).

The first step in assessing a fatigue critical structure is to identify the most critical details to be inspected. Next, the most appropriate inspection type for each location should be selected. The selection of the inspection type depends on the defect type and geometry. Among the available nondestructive inspection techniques, the liquid penetrant inspection, ultrasonic inspection, eddy current inspection, magnetic particle inspection, and acoustic emission inspection are widely used for fatigue crack detection. Each of these methods has its advantages and disadvantages. For instance, the ultrasonic inspection type has a higher probability of detection for embedded cracks; however, it requires a highly experienced inspector (Fisher et al. 1998).

Probability of Detection

The quality of an inspection type can be generally expressed by the probability of detection of a given crack size. The probability of detection has been widely used in the probabilistic inspection and repair planning of structures (Chung et al. 2006; Orcesi and Frangopol 2011). The relationship between the probability of detection and the crack size was investigated by Berens and Hovey (1981), Berens, (1989), and Frangopol et al. (1997). Different forms for this relationship have been proposed such as the shifted exponential, logistic curve, and the lognormal cumulative distribution function (CDF). In this paper, the lognormal CDF is used to represent the probability of detection for different inspection types as a function of the crack size a. The probability of detection PoD is (Crawshaw and Chambers 1984)

$$\text{PoD} = 1 - \Phi\left[\frac{\ln(a) - \lambda}{\beta}\right] \tag{5}$$

where $\Phi(\cdot)$ = standard normal CDF; λ and β, respectively, are the location and scale parameters of the cumulative lognormal PoD curve. The parameters λ and β in Eq. (5) are dependent on the quality of the inspection type.

Probability of Failure at a Critical Detail

In this paper, the probability of failure is considered as the probability that the adopted inspection plan fails to detect an existing crack before it reaches its critical size. This probability can be formulated using the event tree analyses, in which the probabilities of possible inspection outcomes can be evaluated. For a given number of inspections n, the probability of detecting a crack before the failure of the detail can be evaluated as follows (Soliman et al. 2013):

$$PD = \sum_{j=1}^{n} \left\{ \prod_{i=1}^{j} [P(t_{\text{insp},i} \le T_f) \cdot \overline{\text{PoD}}(t_{\text{insp},i-1})] \cdot \text{PoD}(t_{\text{insp},i}) \right\} \tag{6}$$

where $P(t_{\text{insp},i} \le T_f)$ = probability that the ith inspection is performed before the time to failure of the detail T_f; $\text{PoD}(t_{\text{insp},i})$ = probability of detecting the crack at the ith inspection; $\overline{\text{PoD}}(t_{\text{insp},i-1})$ = probability of not detecting the crack at the $(i-1)$th inspection; and $\overline{\text{PoD}}(t_{\text{insp},0}) = 1$ for the first inspection (i.e., $i = 1$). The probability of damage detection at a certain inspection is calculated as a function of the crack size using Eq. (5). Accordingly, the probability of failure can be defined as

$$P_{\text{fail}} = 1 - PD \tag{7}$$

in which P_{fail} represents the probability that the inspection plan will fail to detect an existing crack before it reaches its critical size. The probability P_{fail} is integrated in the proposed framework to find the optimum inspection times.

Expected Total Cost

The expected total cost includes the cost of inspection actions, expected maintenance cost, and the expected failure cost (Mori and Ellingwood 1994). Since the proposed approach does not cover the selection of appropriate maintenance actions, the total cost will be considered as the inspection cost and the expected failure cost. The total inspection cost C_{insp}^{T} can be estimated as

$$C_{\text{insp}}^{T} = \sum_{i=1}^{n} \frac{C_{\text{insp},i}}{(1+r)^{t_{\text{insp},i}}} \tag{8}$$

in which n = number of inspections; $t_{\text{insp},i}$ = application time of the ith inspection; r = annual discount rate of money; and $C_{\text{insp},i}$ = the cost of performing the ith inspection. The cost $C_{\text{insp},i}$ depends on many aspects such as the inspection quality, the location of the inspected detail within the structure, and the time required to perform the inspection, among others.

The failure cost is the cost associated with monetary losses arising from the failure of detecting the damage before reaching the critical state and the consequences of such failure. The expected failure cost is expressed as (Frangopol et al. 1997)

$$E(C_{\text{fail}}) = P_{\text{fail}} \cdot C_{\text{fail}} \tag{9}$$

where P_{fail} = probability of failure calculated using Eq. (7) and C_{fail} = expected monetary losses as a result of the crack reaching its critical size. Accordingly, the total expected cost can be found as

$$E(C_{\text{total}}) = C_{\text{insp}}^{T} + E(C_{\text{fail}}) \tag{10}$$

Integrated Life-Cycle Management Framework

Inspection outcomes provide new information which can be effectively integrated into the management framework to update damage evolution prediction models. In this paper, the new information is considered as the crack size measured during an inspection action. Based on the inspection outcome, a likelihood function is built and combined with the prior knowledge of the model parameters to provide the posterior distributions of the crack growth model parameters. These posterior distributions are used to find an

updated crack growth profile. These steps can be performed many times during the lifetime of the structure, where the previous knowledge, as well as the current inspection outcomes, can be incorporated to find the future crack growth. However, in this paper, this process will be performed before implementing the inspection plan. Possible inspection outcomes will be evaluated and integrated into the management plan such that effective actions can be taken. Having the results of this framework ready beforehand allows for immediate decision making based on the inspection results. The detailed flowchart of the proposed framework is given in Fig. 2. As shown, the life-cycle management framework starts with an input of the deterioration model parameters. These parameters include material properties and loading conditions. Needless to say, available structural health monitoring (SHM) data can improve the quality of the management process, especially for evaluating the loading conditions at the studied location (Frangopol 2011). The inputs also includes the damage thresholds, inspection type parameters, and the cost data.

Next, the damage evolution profile with time is constructed. In this paper, Monte Carlo simulation is used to find the crack growth profiles. Based on these profiles, the optimum inspection times which yield the minimum total cost are found. The probability density function (PDF) of the predicted crack size at the time of inspection is then evaluated using the simulation results and a set of inspection outcome possibilities are defined. The updating process is performed based on the defined inspection outcomes and posterior distributions of model parameters are used to find the updated damage propagation profiles. Crack size thresholds are defined for selecting the appropriate management actions based on inspection outcomes. In this paper, management actions are built upon crack size thresholds as follows: (1) perform future inspection for $a_I \leq a_{\text{insp},i} \leq a_{II}$, (2) perform immediate repair and reassessment for $a_{\text{insp},i} \geq a_{II}$, and (3) perform reassessment for $a_{\text{insp},i} \leq a_I$, where $a_{\text{insp},i}$ is the crack size measured at the ith inspection, and a_I, a_{II} are the crack size thresholds for determining the appropriate management actions by considering the difference

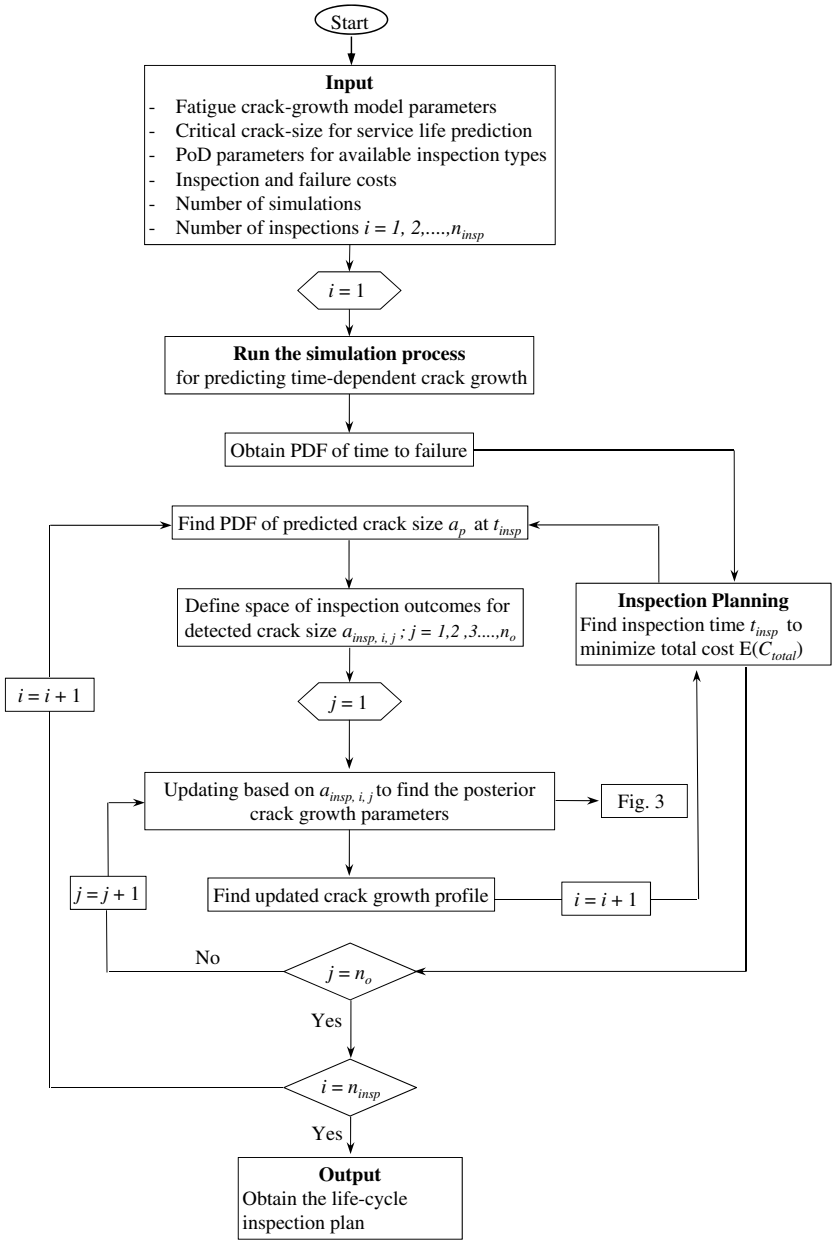

Fig. 2. Flowchart of management framework

J. Infrastruct. Syst. 2014.20.

between the crack size measured during inspection and the one predicted at the time of inspection. The allowable difference can be determined depending on the importance of the damaged detail within the structure. A detail with high importance would require an increased damage prediction accuracy and, in turn, a smaller allowable difference between the measured and the predicted crack sizes; thus, creating closer thresholds. In this paper, these thresholds are determined in terms of the descriptors of the PDF of the predicted crack size at the time of inspection. The result of this process is an interactive management plan which gives the manager a deeper insight into the safety level and the remaining service life based on the crack size measured at a certain inspection.

Bayesian Updating of Model Parameters

In this paper, the Bayesian approach is employed to update the crack growth model parameters. This process reduces the uncertainties in the model parameters and leads to a more accurate damage prediction process. The prior knowledge about the model parameters can be combined with the new information resulting from inspection actions to yield the posterior distribution of model parameters as

$$P(\boldsymbol{\theta}|\mathbf{d}) = \frac{P(\boldsymbol{\theta}) \cdot P(\mathbf{d}|\boldsymbol{\theta})}{\int P(\boldsymbol{\theta}) \cdot P(\mathbf{d}|\boldsymbol{\theta}) d\boldsymbol{\theta}} \tag{11}$$

where $P(\boldsymbol{\theta}|\mathbf{d})$ = posterior distribution of model parameters $\boldsymbol{\theta}$ given additional information $\mathbf{d}$; $P(\boldsymbol{\theta})$ = prior distribution of model parameters; $P(\mathbf{d}|\boldsymbol{\theta})$ = likelihood function of obtaining information $\mathbf{d}$ conditioned by $\boldsymbol{\theta}$; and $\mathbf{d}$ and $\boldsymbol{\theta}$ are the vectors of observed data and model parameters, respectively. In this case, the vector of observed data contains crack sizes obtained during inspections as

$$d = \{a_{\text{insp},1}, a_{\text{insp},2}, \ldots, a_{\text{insp},n}\} \tag{12}$$

where $a_{\text{insp},i}$ = measured crack size at the ith inspection and n = number of inspections. In Eq. (11), $\int P(\boldsymbol{\theta}) \cdot P(\mathbf{d}|\boldsymbol{\theta}) d\boldsymbol{\theta}$ represents a normalizing constant which can be dropped (Martinez and Martinez 2002) leading to

$$P(\boldsymbol{\theta}|\mathbf{d}) \propto P(\boldsymbol{\theta}) \cdot P(\mathbf{d}|\boldsymbol{\theta}) \tag{13}$$

The prior distributions of the crack growth model parameters can be found based on the material properties. In this study, the distributions of the material crack growth parameters m, C, and the initial crack size a_o are updated using the discussed approach. The likelihood function of obtaining field measurements $\mathbf{d}$ given the model parameters $\boldsymbol{\theta}$ can be expressed as (Perrin et al. 2007)

$$P(\mathbf{d}|\boldsymbol{\theta}) = \prod_{i=1}^{n} \left\{ \frac{1}{\sqrt{2\pi} \cdot \sigma_e} \cdot \exp\left[-\frac{1}{2} \left(\frac{d_i - a_{p,i}}{\sigma_e} \right)^2 \right] \right\} \tag{14}$$

where d_i and $a_{p,i}$ are the observed and predicted data, respectively, at the ith inspection; σ_e represents a single error term combining the measurement and modeling errors which is assumed to follow a normal distribution with zero mean and a standard deviation σ_e (i.e., $N(0, \sigma_e)$).

By knowing the likelihood function and the prior distribution of the model parameters, the posterior distribution of the model parameters can be found by using Markov chain Monte Carlo simulation. The Metropolis algorithm (Metropolis et al. 1953) is employed herein to draw samples from the posterior distribution when the chain has converged. Those samples can be used as an approximation for the target posterior distribution.

Metropolis Algorithm

The Metropolis method (Metropolis et al. 1953) used in this study is a special case of the Metropolis-Hasting algorithm (Hasting 1970). The algorithm obtains the state of a chain $\boldsymbol{\theta}_{t+1}$ by sampling a candidate vector $\boldsymbol{\theta}^*$ from a proposed distribution $q(\boldsymbol{\theta}^*|\boldsymbol{\theta}_t)$ that depends only on the previous state of the chain $\boldsymbol{\theta}_t$. The proposal distribution for the Metropolis method is symmetric, in which the candidate vector is accepted as the next state of the chain with probability

$$\alpha(\boldsymbol{\theta}_t, \boldsymbol{\theta}^*) = \min\left[1, \frac{P(\boldsymbol{\theta}^*|\mathbf{d}) q(\boldsymbol{\theta}_t|\boldsymbol{\theta}^*)}{P(\boldsymbol{\theta}_t|\mathbf{d}) q(\boldsymbol{\theta}^*|\boldsymbol{\theta}_t)}\right] \tag{15}$$

where the proposal distribution cancel out due to symmetry (i.e., $q(\boldsymbol{\theta}_t|\boldsymbol{\theta}^*) = q(\boldsymbol{\theta}^*|\boldsymbol{\theta}_t)$). The random generation here adopts a random walk algorithm, in which $\boldsymbol{\theta}_{t+1} = \boldsymbol{\theta}_t + \zeta$, where ζ is a Gaussian noise parameter.

Thus the acceptance probability is

$$\alpha(\boldsymbol{\theta}_t, \boldsymbol{\theta}^*) = \min\left[1, \frac{P(\boldsymbol{\theta}^*) \cdot P(\mathbf{d}|\boldsymbol{\theta}^*)}{P(\boldsymbol{\theta}_t) \cdot P(\mathbf{d}|\boldsymbol{\theta}_t)}\right] \tag{16}$$

The flowchart of the adopted algorithm is shown in Fig. 3. Since the first n_b sample may not represent the posterior distribution, the convergence of the chain has to be monitored (Gelman 1996). Convergence monitoring determines when the chain is considered safe to represent the target posterior distribution. In this paper, a method proposed by Gelman (1996) is used, in which multiple parallel chains are used with different starting points and the convergence to the target distribution is evaluated by calculating the

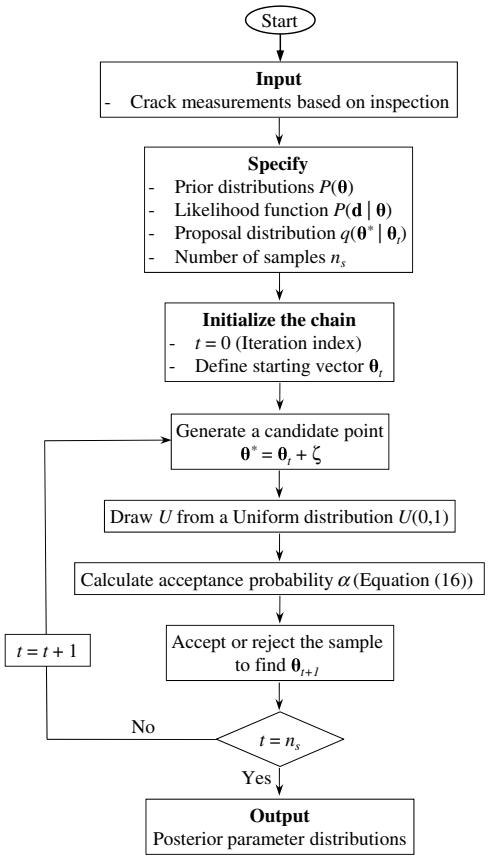

Fig. 3. Flowchart of the updating Markov chain Monte Carlo simulation

estimated potential scale reduction factor $\hat{R}$. This factor, given by the ratio of the overall variance $v\hat{a}r(\nu)$ to the within-sequence variance W, is expressed as

$$\hat{R} = \frac{v\hat{a}r(\nu)}{W} \tag{17}$$

where υ is the scalar summary of interest (such as the mean value and standard deviation of the underlying random variables). It is sufficient to run the sequence until a value of 1.1 or 1.2 for $\hat{R}$ is reached (Gelman 1996). However, for multivariate chains, higher values of $\hat{R}$ can be used (Brooks and Gelman 1998). In this paper, two parallel chains are used to sample from the posterior distribution and convergence is considered to occur when the value of $\hat{R}$ for all the scalar summaries drops below 1.2. Hence, the first n_b samples generated before convergence, which correspond to the burn-in period, are discarded.

Illustrative Example

The proposed management plan is illustrated on a steel ship side shell detail subjected to fatigue. The side shell structure is known to have multiple fatigue critical locations that need to be inspected frequently (Ma et al. 1999). At these locations, the stress cycles are caused by the fluctuating hydrodynamic pressures as well as the pressure induced by waves. Another possible critical location is the intersection of bottom longitudinal stiffeners with transverse web frames (Glen et al. 1999). At this location, the fluctuating stress is mainly caused by the hull girder bending. The critical location considered in this example and shown in Fig. 4 is the joint between the transverse frame and the longitudinal stiffener. In this example, the initial crack size a_o is assumed to follow a normal distribution with a mean of 0.5 mm and a coefficient of variation (COV) = 0.1. The material crack growth coefficient C is considered to follow a lognormal distribution with a mean = 2.3×10^{-12} (British Standards Institution 2005), using units of mm/cycle for crack growth rate and $\text{N/mm}^{3/2}$ for the stress intensity factor range, and a COV = 0.3 while the parameter m is assumed to follow a normal distribution with a mean = 3.0 and a COV = 0.1. The correlation coefficient between the natural logarithm of the parameter C [i.e., $\ln(C)$] and m is considered to be −0.9 (Cremona 1996). The stress range S_{re} is considered as a random variable following a Weibull distribution and the geometry function $G(a)$ is considered to be constant = 1.12 (Guedes Soares and Garbatov 1999). The critical crack size is assumed herein to be 50 mm. Descriptors of different parameters adopted for the crack size prediction are given in Table 1.

Based on Eq. (4), Monte Carlo simulation is performed with 100,000 samples to find the time required to reach the critical crack size. Fig. 5 shows the results of the Monte Carlo simulation, in which the mean and standard deviation of the time required to reach different crack sizes are provided with the PDF of the time to reach a crack size of 10, 20, 30, 40 mm, and the critical crack size of 50 mm. As shown in Fig. 5, the mean value of the time to failure T_f (i.e., time to reach the critical crack size) is 22.7 years and the standard deviation is 10.81 years. The number of samples for the Monte Carlo simulation is selected based on extensive convergence analyses in which the simulation results were found to stabilize before the selected number of simulations. A sample of the convergence analyses is shown in Fig. 6.

Optimum Inspection Times

The scheduling to find optimum inspection times is formulated as an optimization problem with the objective of minimizing the expected total cost $E(C_{\text{total}})$ as follows:

$$\text{Find } t_{\text{insp},1}, t_{\text{insp},2}, t_{\text{insp},3}, \ldots, t_{\text{insp},n} \tag{18}$$

$$\text{to minimize } E(C_{\text{total}}) \tag{19}$$

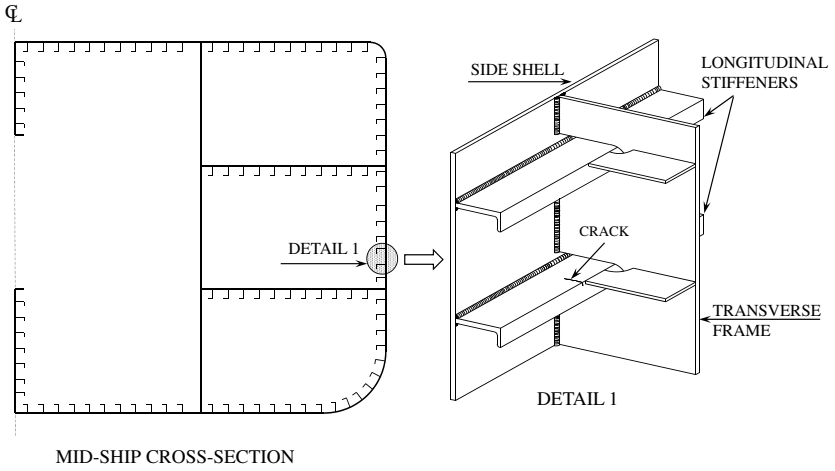

Fig. 4. Midship cross section and the studied critical location

Table 1. Random Variables for Crack-Growth Prediction and Their Parameters

Random variable	Notation (units)	Mean	Coefficient of variation	Distribution type
Initial crack size	a_o (mm)	0.5	0.1	Normal
Material crack-growth parameters	m	3.0	0.1	Normal
	C	2.3×10^{-12}	0.3	Lognormal
Stress range	S_{re} (MPa)	22.5	0.1	Weibull
Annual number of cycles	N_{av} (cycles/year)	1.0×10^6	0.1	Lognormal

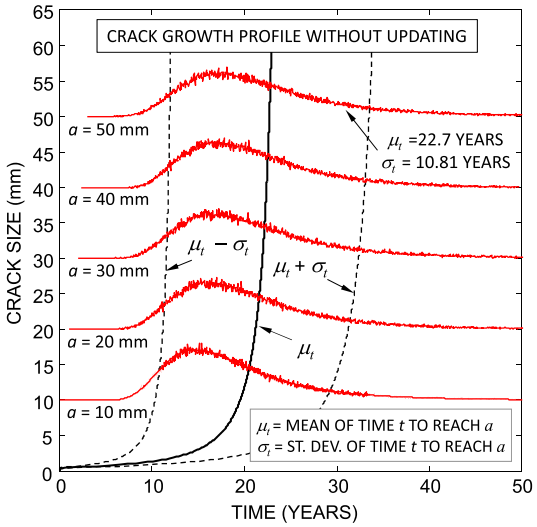

Fig. 5. Time-variant crack size with the PDF of time to reach a size of 10, 20, 30, 40, and 50 mm

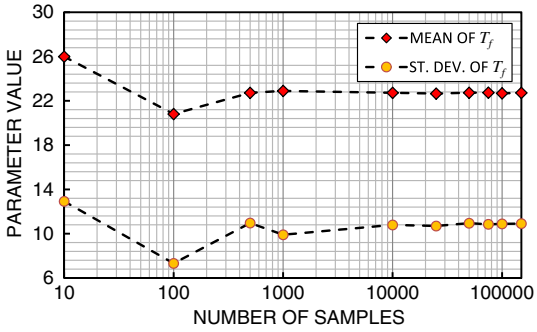

Fig. 6. A sample of convergence analyses of the fatigue crack growth simulation process

$$\text{such that } t_{\text{insp},i} - t_{\text{insp},i-1} \geq 1.0 \text{ year} \tag{20}$$

$$\text{given } n, \boldsymbol{\Psi}, C_{\text{fail}}, \mathbf{C}_{\text{insp}}, r \quad \text{and the PDF of } T_f \tag{21}$$

where $t_{\text{insp},i} = i$th inspection time; $E(C_{\text{total}})$ = expected total cost as given by Eq. (10); n = number of inspections; $\boldsymbol{\Psi}$ = matrix consisting of the PoD parameters λ and β for different available inspection types; $\mathbf{C}_{\text{insp}}$ = vector consisting of the cost of performing a single inspection using each of the available inspection types; C_{fail} = expected monetary losses as a result of the crack reaching its critical size without being detected by inspection; and r = annual discount rate of money assumed 2%. The PDF of the time to failure T_f is obtained from the results of the Monte Carlo simulation process. As shown by Eq. (20), the minimum time interval between consecutive inspection actions is set to be 1.0 year.

For this example, three inspection types are considered, namely, the eddy current inspection (ECI), the ultrasonic inspection (UI), and the liquid penetrant inspection (LPI). The ratio between relative inspection costs for the three respective inspection types and the cost of failure, $C_{\text{insp,ECI}}$:$C_{\text{insp,UI}}$:$C_{\text{insp,LPI}}$:C_{fail}, is considered to be $5.0{:}4.0{:}3.0{:}1 \times 10^3$. The PoD parameters λ and β for each of the inspection types are shown in Table 2. These adopted PoD parameters are deduced based on the inspection practices of the aerospace industry (Forsyth and Fahr 1998) and are used here for illustrative purposes. This optimization problem is solved using the optimization toolbox provided in *MATLAB version R2011a* (MathWorks Inc. 2011). In this manner, the optimum inspection times for a given inspection type are found.

Fig. 7 shows the optimum inspection schedule for one (i.e., Schedules A, B, and C) and two scheduled inspections (i.e., Schedules D, E, and F) with inspection types of different qualities defined by the factors λ and β. For the case of the two inspections, the shown times of the second scheduled inspections are independent of the results of the previous inspection (i.e., updating process is not utilized). As shown in Fig. 7, the one scheduled inspection should be performed after 9.09, 12.38, and 14.95 years of service for ECI, UI, and LPI, respectively. For the case of two scheduled inspections, the first inspection is planned to be performed at 6.92, 10.3, and 12.72 years for the three respective inspection types. At the first inspection associated with Schedules D, E, and F, the mean predicted crack sizes are found by the Monte Carlo simulation to be 1.04 mm, 1.92 mm, and 2.95 mm, respectively. Optimum inspection schedules and their associated objective function values are given in Table 2.

Updated Inspection Schedules and Damage Evolution Profiles

Based on the outcomes of the first scheduled inspection, the model parameters, and accordingly, the crack growth profiles are updated. Considering inspection Schedule D, which has the highest quality of inspection, the first inspection is scheduled after 6.92 years in service. At this time, the mean of the predicted crack size $E[a_p(t_{\text{insp},1})]$ is found to be 1.04 mm. Accordingly, the crack size threshold for reassessment a_I is considered to be $0.5 \cdot E[a_p(t_{\text{insp},1})]$, while the threshold a_{II} for the repair and reassessment of the inspected location is taken as $1.5 \cdot E[a_p(t_{\text{insp},1})]$, yielding approximately 0.5 mm and 1.5 mm for a_I and a_{II}, respectively. For a measured crack size significantly smaller than the predicted one, a reassessment is recommended to find the reason behind the large difference between the results. This reassessment

Table 2. Design Variables and Objective Function Values Associated with the Optimum Solutions

Number of inspections	Inspection schedule	Inspection method	PoD parameters (Forsyth and Fahr 1998)		Relative cost	Inspection times (years)		Objective value
			λ	β	C_{insp}:C_{fail}	$t_{\text{insp},1}$	$t_{\text{insp},2}$	$E(C_{\text{total}})$
$n = 1$	A	ECI	−0.968	−0.571	$5.0{:}1 \times 10^3$	9.09	—	35.16
	B	UI	0.122	−0.305	$4.0{:}1 \times 10^3$	12.38	—	195.19
	C	LPI	0.829	−0.423	$3.0{:}1 \times 10^3$	14.95	—	412.02
$n = 2$	D	ECI	−0.968	−0.571	$5.0{:}1 \times 10^3$	6.92	9.9	11.84
	E	UI	0.122	−0.305	$4.0{:}1 \times 10^3$	10.3	14.77	110.48
	F	LPI	0.829	−0.423	$3.0{:}1 \times 10^3$	12.72	17.9	310.45

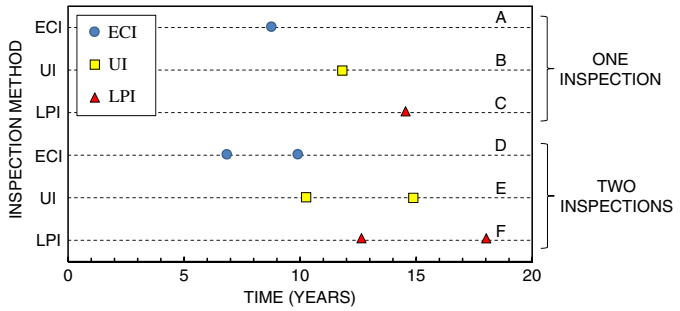

Fig. 7. Optimum schedules for the adopted inspection types

may result in finding different loading conditions in terms of the stress ranges or the number of loading cycles acting on the detail. Moreover, it may indicate different crack conditions (e.g., crack geometry or orientation) than those used in the prediction process. On the other hand, for crack sizes larger than a_{II}, repair and reassessment would be recommended to maintain the safety of the structure against sudden failures that may occur due to the unstable growth of the existing crack.

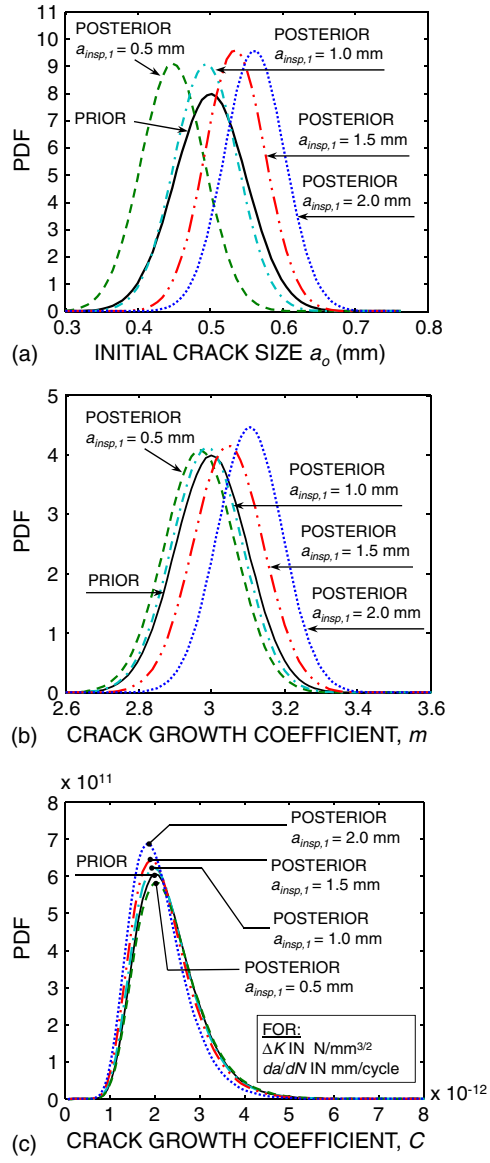

Fig. 8. Prior and posterior distributions of model parameters based on detected crack sizes at the first inspection: (a) initial crack size, a_o; (b) crack growth coefficient, m; (c) crack growth coefficient, C

The updating process for the studied range is performed using Eq. (11) and the Metropolis algorithm discussed earlier in this paper. The three crack growth parameters a_o, m, and C are updated in this procedure where the parameter σ_e is assumed to be 0.2mm (Perrin et al. 2007). Fig. 8 shows the prior and posterior distributions of the three updated parameters for selected measured crack sizes at the time of the first scheduled inspection (i.e., 6.92 years). Two parallel chains are used simultaneously to monitor the convergence of the simulation process and the first n_b samples corresponding to the burn-in period are neglected. Fig. 9 shows the evolution of the $\hat{R}$ values for the different descriptors of the updated random variables. As a further check of the sampling convergence, the slice sampling technique (Neal 2003) was also used and it was found to provide matching results to those obtained by the Metropolis algorithm. For the slice sampling, the *MATLAB R2011a* statistical tool box (MathWorks Inc. 2011) built-in sampling function was used to sample from the posterior distribution of the parameters. This algorithm, in its simplest form, draws the samples by selecting a horizontal slice at a vertical level drawn uniformly from the region under the function. The next sample which lies under the function is drawn uniformly from this horizontal slice (Neal 2003). The slice sampling technique does not require the definition of a proposal function which makes it favorable in many cases where the proposal function is difficult to obtain. Based on the posterior crack growth parameters resulting from the Metropolis algorithm, updated damage evolution profiles are obtained.

Fig. 10(a) shows the updated profiles of the mean time required to reach different crack sizes and Fig. 10(b) shows the updated PDFs of the time to failure for different crack sizes detected at the first inspection. The same updating approach is applied to inspection schedules E and F where the UI and LPI are respectively used. For the UI, the first inspection is scheduled after 10.3 years of service and the thresholds a_I and a_{II} are considered to be 1.0 mm and 3.0 mm, respectively. The mean of the updated crack growth profiles for this case are shown in Fig. 11(a), while the updated PDFs of the time to failure for different detected crack sizes are shown in Fig. 11(b). Similarly, Figs. 12(a and b) show updated

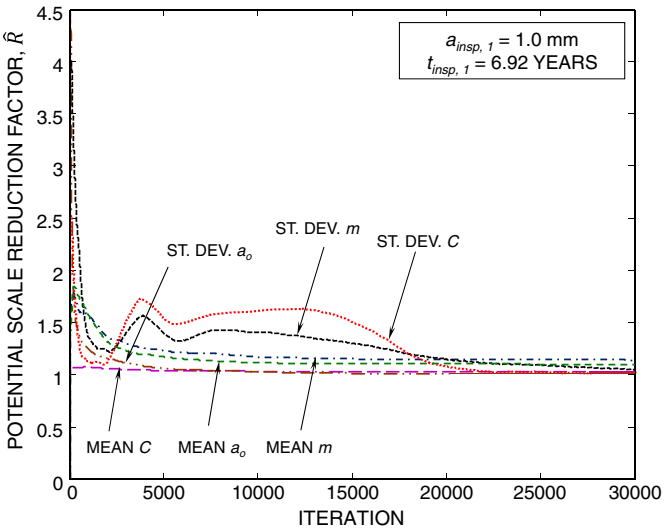

Fig. 9. Evolution of $\hat{R}$ for the scalar summaries in the Markov chain Monte Carlo simulation process

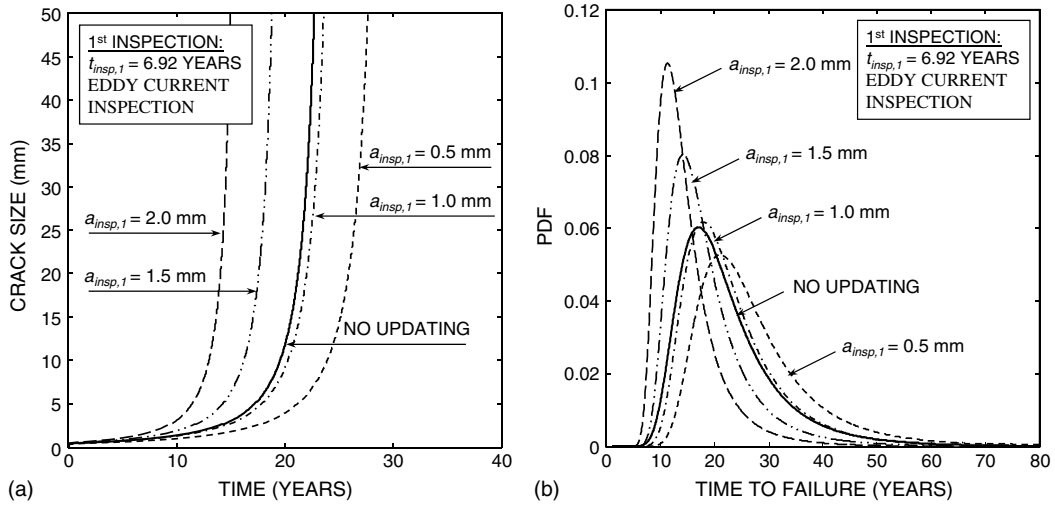

Fig. 10. Updated results for different crack sizes measured at first inspection ($t_{\text{insp},1} = 6.92$ years): (a) updated mean of crack growth profiles; (b) updated PDFs of the time to failure

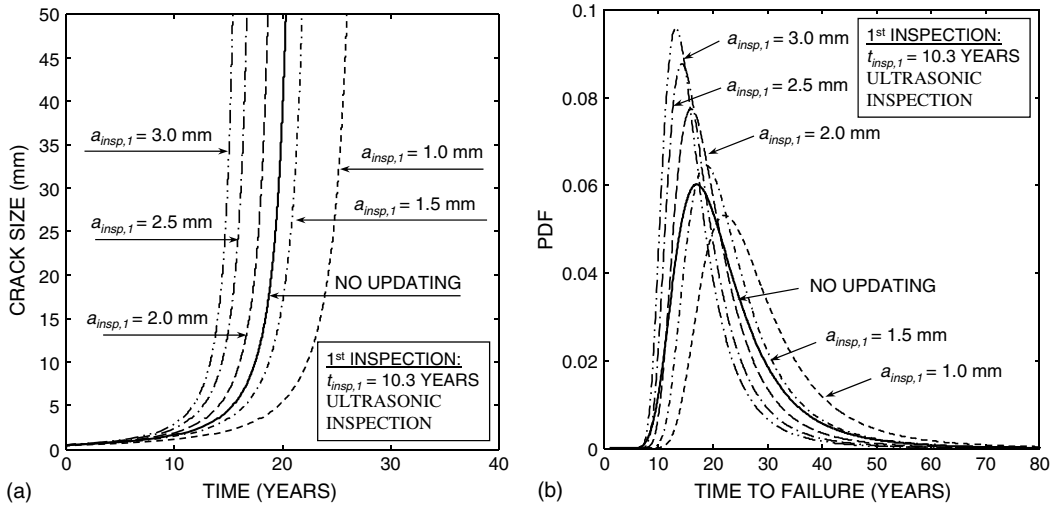

Fig. 11. Updated results for different crack sizes measured at first inspection ($t_{\text{insp},1} = 10.3$ years): (a) updated mean of crack growth profiles; (b) updated PDFs of the time to failure

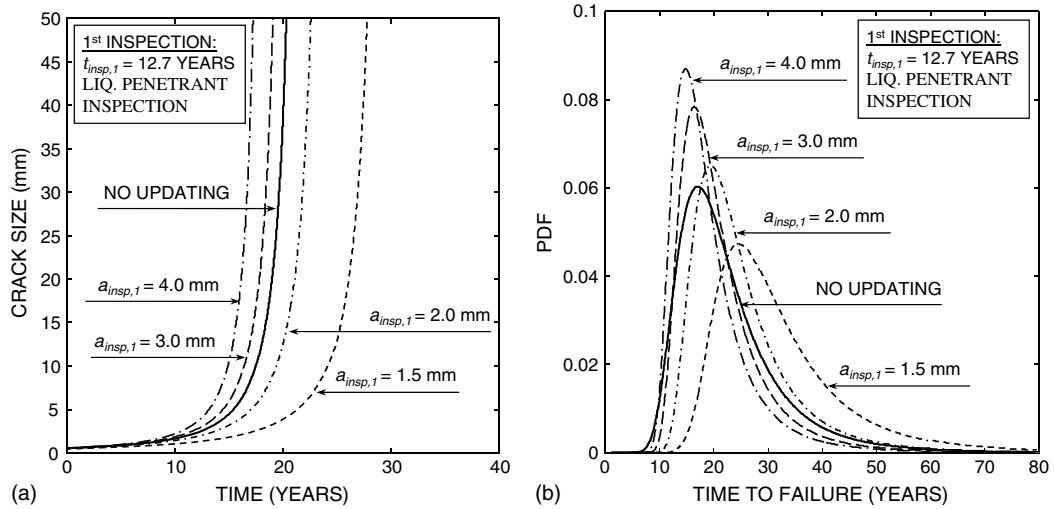

Fig. 12. Updated results for different crack sizes measured at first inspection ($t_{\text{insp},1} = 12.7$ years): (a) updated mean of crack growth profiles; (b) updated PDFs of the time to failure

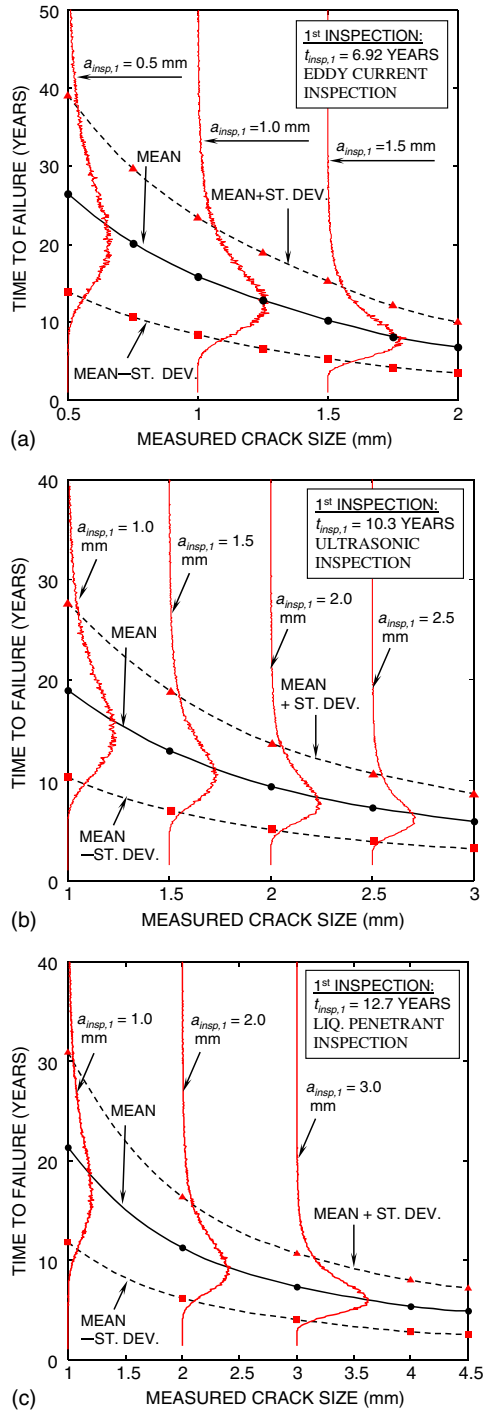

Fig. 13. Remaining fatigue life with respect to the measured crack size at first inspection: (a) first inspection performed at 6.92 years; (b) first inspection performed at 10.3 years; (c) first inspection performed at 12.7 years

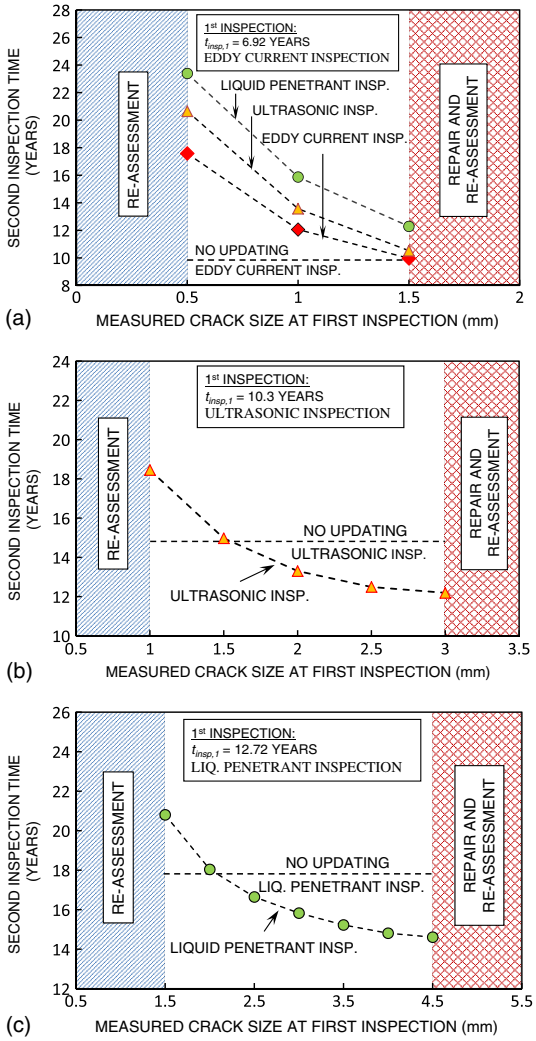

Fig. 14. Second inspection times for different crack sizes measured at first inspection: (a) ECI for first inspection and ECI, UI, and LPI for second inspection; (b) UI for first and second inspections; (c) LPI for first and second inspections

crack growth profiles and the updated PDFs of the fatigue service life, respectively, for the LPI performed at 12.72 years of service life. Figs. 13(a–c) show, for the three inspection strategies, the descriptors (i.e., mean and standard deviation) of the remaining fatigue life for different measured crack sizes at the first inspection along with the PDF of the remaining fatigue life for selected outcomes of the first inspection.

The next step is to find the optimum time of the second inspection based on the second inspection type and the outcomes of the first inspection. This is performed using the optimization approach given by Eqs. (18)–(21) for one scheduled inspection (i.e., $n = 1$). For the ECI performed at 6.92 years, the optimum times for second inspection using the eddy current technique are given in Fig. 14(a) for different first inspection outcomes. Additionally, the inspection time resulting from the optimization process without updating (i.e., $t_{\text{insp},2} = 9.9$ years) is plotted. As shown in the figure, inspection times are significantly affected by the previous inspection outcomes. The approach can also consider scheduling the second inspection with a different inspection type. Combining inspection types in a management plan where higher quality inspections are performed earlier and lower quality inspections are performed later can be effective since inspection types with a lower quality will have an acceptable ability to detect the damage when performed later in life (i.e., with higher damage levels). Accordingly, times for the second inspection using the ultrasonic and liquid penetrant techniques are calculated and shown in Fig. 14(a). Figs. 14(b and c) show the times for performing UI and LPI, respectively, in both the first and second inspection. Updated second inspection times for different types of inspections are given in Table 3 along with the predicted parameters of the remaining fatigue life after the first inspection.

Table 3. Remaining Fatigue Life and Optimum Times for the Second Inspection Based on the Measured Crack Size at First Inspection

Inspection type	First inspection time $t_{\text{insp},1}$ (years)	Mean of predicted crack size at first inspection $a_p(t_{\text{insp},1})$ (mm)	Measured crack size at first inspection $a_{\text{insp},1}$ (mm)	Mean of remaining fatigue life (years)	Standard deviation of remaining fatigue life (years)	Time interval between inspections $t_{\text{insp},2} - t_{\text{insp},1}$ (years)	Second inspection time $t_{\text{insp},2}$ (years)
Eddy current	6.92	1.04	0.5	26.48	12.63	10.66	17.58
			1.0	15.94	7.55	5.14	12.06
			1.5	10.19	4.95	3.05	9.97
Ultrasonic	10.30	1.92	1.0	18.98	8.73	8.15	18.45
			1.5	13.00	5.99	4.67	14.97
			2.0	9.38	4.31	3.30	13.6
			2.5	7.29	3.42	2.19	12.49
			3.0	5.89	2.76	1.89	12.19
Liquid penetrant	12.72	2.95	1.5	15.43	9.59	8.08	20.8
			2.0	11.24	5.09	5.32	18.04
			2.5	8.73	3.97	3.92	16.64
			3.0	7.35	3.34	3.11	15.83
			3.5	6.22	2.92	2.51	15.22
			4.0	5.37	2.60	2.09	14.81
			4.5	4.87	2.31	1.89	14.61

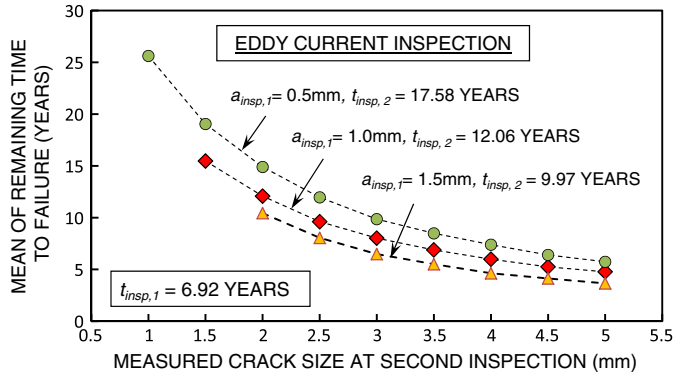

Fig. 15. Mean of the remaining fatigue life based on the crack size measured at the second inspection for multiple outcomes of the first inspection

The procedure can also be used to find the remaining fatigue life after n inspections with specified outcomes. Fig. 15 shows the remaining fatigue life after the second inspection based on the crack size measured during the first and second inspection. For this process, the Metropolis algorithm uses the likelihood function with a number of inspections $n = 2$ where the second inspection outcome is chosen to cover a range of $a_{\text{insp},1} + 0.5$ mm up to 5.0 mm. Similar profiles covering different inspection types and outcomes after the second inspection can be plotted. This information about the remaining fatigue life, along with the required safety levels and available budget, can help the decision maker to effectively plan for future repair actions.

Conclusions

This paper presents a probabilistic approach for finding a comprehensive management plan for fatigue-sensitive structures. This plan gives the time of the first inspection, and based on the inspection outcome and the predicted crack size, appropriate management actions are specified. These actions include reassessing the detail, proposing a time for the second inspection action, or performing repair. The proposed approach uses the Markov chain Monte Carlo method applied through the Metropolis algorithm to find the updated crack growth parameters after each inspection. Three parameters, namely, the initial crack size a_o, and material constants m and C are updated after each inspection. The posterior parameters are used next to find the updated time to failure and the next inspection times that fulfill the optimization goals. The approach is automated in a *MATLAB* environment and is found to be computationally feasible using parallel processing. The computational time is significantly affected by the sampling method adopted for updating the model parameters. Other factors such as the geometry and type of fatigue crack and the optimization technique also affect the computational effort. Convergence is monitored throughout the updating process by running multiple parallel chains and checking the variance within the chain and the overall variance. The result of this process is a comprehensive life-cycle inspection plan that can be directly implemented on the structure and gives the manager the ability to make real-time decisions based on the inspection outcomes. The following conclusions are drawn:

1. Using the proposed framework, management plans allowing for real-time decisions based on future inspection outcomes can be developed. The outcomes of such plans are the next inspection times and the damage level-based thresholds for reassessment and repair decisions;
2. The proposed life-cycle management framework is general and can cover additional types of time-dependent deteriorating mechanisms such as corrosion and corrosion-induced fatigue;
3. Different optimization techniques for inspection scheduling can be included in this framework according to the management's needs. These goals may include extending the service life as an objective; however, care should be taken in selecting the optimization technique as it may significantly affect the computational effort; and
4. The proposed model can be extended to include the repair method as an outcome by defining crack size-based thresholds for different repair actions.

Acknowledgments

The support by grants from (1) the National Science Foundation (NSF) Award CMS-0639428, (2) the Commonwealth of Pennsylvania, Department of Community and Economic Development, through the Pennsylvania Infrastructure Technology Alliance (PITA), (3) the U.S. Federal Highway Administration (FHWA)

Cooperative Agreement Award DTFH61-07-H-00040, (4) the U.S. Office of Naval Research (ONR) Awards N00014-08-1-0188 and N00014-12-1-0023, and (5) the National Aeronautics and Space Administration (NASA) Award NNX10AJ20G is gratefully acknowledged. The opinions and conclusions presented in this paper are those of the authors and do not necessarily reflect the views of the sponsoring organizations.

References

Berens, A. P. (1989). "NDE reliability data analysis." *Metal handbook*, 9th Ed., Vol. 17, ASM Int., Material Park, OH, 689–701.

Berens, A. P., and Hovey, P. W. (1981). "Evaluation of NDE reliability characterization." *Air force Wright-aeronautical laboratory*, Wright-Patterson Air Force Base, Dayton, OH.

British Standards Institution (BSI). (2005). "Guidance on methods for assessing the acceptability of flaws in fusion welded structures," *BS7910*, London.

Brooks, S., and Gelman, A. (1998). "General methods for monitoring convergence of iterative simulations." *J. Comput. Graph. Stat.*, 7(4), 434–455.

Chung, H.-Y., Manuel, L., and Frank, K. H. (2006). "Optimal inspection scheduling of steel bridges using nondestructive testing techniques." *J. Bridge Eng.*, 10.1061/(ASCE)1084-0702(2006)113(305), 305–319.

Cramer, E. H., and Bea, R. G. (1991). "Fatigue reliability model for inspection, updating and repair of welded geometries." *Marine Structural Inspection, Maintenance, and Monitoring Symp.*, Ship Structure Committee, Washington, DC.

Cramer, E. H., and Friis-Hansen, P. (1994). "Reliability-based optimization of multi-component welded structures." *J. Offshore Mech. Arctic Eng.*, 116(4), 223–238.

Crawshaw, J., and Chambers, J. (1984). *A concise course in a-level statistics*, Stanley Thornes, Cheltenham, U.K.

Cremona, C. (1996). "Reliability updating of welded joints damaged by fatigue." *Int. J. Fatigue*, 18(8), 567–575.

Das, P. C. (2000). "Reliability based bridge management procedures." *Bridge Management 4: Inspection, maintenance, assessment and repair*, M. J. Ryall, G. A. R. Parke and J. E. Harding, eds., Thomas Telford Publishing, London, 1–11.

Enright, M. P., and Frangopol, D. M. (1999). "Maintenance planning for deteriorating concrete bridges." *J. Struct. Eng.*, 10.1061/(ASCE)0733-9445(1999)125:12(1407), 1407–1414.

Estes, A. C., and Frangopol, D. M. (2001). "Minimum expected cost—oriented optimal maintenance planning for deteriorating structures: application to concrete bridge decks." *Reliab. Eng. Syst. Saf.*, 73(3), 281–291.

Fisher, J. W. (1984). *Fatigue and fracture in steel bridges, case studies*, Willey, New York.

Fisher, J. W., Kulak, G. L., and Smith, I. F. (1998). *A fatigue primer for structural engineers*, American Institute of Steel Construction, Chicago, IL.

Forsyth, D. S., and Fahr, A. (1998). "An evaluation of probability of detection statistics." *RTO-AVT Workshop on Airframe Inspection Reliability under Field/Depot Conditions*, NATO Research and Technology Organization, Neuilly-sur-Seine, Cedex, France.

Frangopol, D. M. (2011). "Life-cycle performance, management, and optimisation of structural systems under uncertainty: accomplishments and challenges." *Struct. Infra. Eng.*, 7(6), 389–413.

Frangopol, D. M., Lin, K. Y., and Estes, A. C. (1997). "Life-cycle cost design of deteriorating structures." *J. Struct. Eng.*, 10.1061/(ASCE)0733-9445(1997)123:10(1390), 1390–1401.

Garbatov, Y., and Guedes Soares, C. (2001). "Cost and reliability based strategies for fatigue maintenance planning of floating structures." *Reliab. Eng. Syst. Saf.*, 73(3), 293–301.

Gelman, A. (1996). "Inference and monitoring convergence." *Markov chain Monte Carlo in practice*, W. R. Gilks, S. Richardson and D. T. Spiegelhalter, eds., Chapman and Hall, London, 131–143.

Glen, I. F., Dinovitzer, A., Paterson, R. B., Luznil, L., and Bayley, C. (1999). "Fatigue-resistant detail design guide for ship structures." *Ship Structure Committee Rep. No. SSC–405*, Ship Structure Committee, Washington, DC.

Guedes Soares, C., and Garbatov, Y. (1999). "Reliability based fatigue design of maintained welded joints in the side shell of tankers." *Fatigue Design and Reliability, European Structural Integrity Society*, G. Marquis, and J. Solin, eds., 23, Elsevier, Amsterdam, 13–28.

Hasting, W. K. (1970). "Monte Carlo sampling methods using Markov chains and their applications." *Biometrika*, 57(1), 97–109.

Heredia-Zavoni, E., and Montes-Iturrizaga, R. (2004). "A Bayesian model for the probability distribution of fatigue damage in tubular joints." *J. Offshore Mech. Arctic Eng.*, 126(3), 243–249.

Kale, A. A., and Haftka, R. T. (2008). "Tradeoff of weight and inspection cost in reliability-based structural optimization." *J. Aircraft*, 45(1), 77–85.

Kim, S., and Frangopol, D. M. (2011). "Optimum inspection planning for minimizing fatigue damage detection delay of ship hull structures." *Int. J. Fatigue*, 33(3), 448–459.

Kim, S., Frangopol, D. M., and Soliman, M. (2013). "Generalized probabilistic framework for optimum inspection and maintenance planning." *J. Struct. Eng.*, 10.1061/(ASCE)ST.1943-541X.0000676, 435–447.

Kwon, K., and Frangopol, D. M. (2011). "Bridge fatigue assessment and management using reliability-based crack growth and probability of detection models." *Probabilist. Eng. Mech.*, 26(3), 471–480.

Li, Z., Zhang, Y., and Wang, C. (2013). "A sensor-driven structural health prognosis procedure considering sensor performance degradation." *Struct. Infra. Eng*, 9(8), 764–776.

Ma, K.-T., Orisamolu, I. R., and Bea, R. G. (1999). "Optimal strategies for inspection of ships for fatigue and corrosion damage." *Ship Structure Committee Rep. No. SSC–407*, Ship Structure Committee, Washington, DC.

Madsen, H. O., Skjong, R. K., Tallin, A. G., and Kirkemo, F. (1987). "Probabilistic fatigue crack growth analysis of offshore structures, with reliability updating through inspection." *Marine Structural Reliability Symp.*, Arlington, VA.

Madsen, H. O., Torhaug, E., and Cramer, E. H. (1991). "Probability-based cost benefit analysis of fatigue design, inspection, and maintenance." *Marine Structural Inspection, Maintenance, and Monitoring Symp.*, Ship Structure Committee, Arlington, VA.

Martinez, W. L., and Martinez, A. R. (2002). *Computational statistics handbook with MATLAB*, Chapman & Hall/CRC, Boca Raton, FL.

MathWorks. (2011). *Optimization toolbox 6 user's guide*, The MathWorks, Natick, MA.

Metropolis, N., Rosenbluth, A., Rosenbluth, M., Teller, A., and Teller, E. (1953). "Equation of state calculations by fast computing machines." *J. Chem. Phys.*, 21(6), 1087–1092.

Moan, T., and Song, R. (2000). "Implications of inspection updating of system fatigue reliability of offshore structures." *J. Mech. Arct. Eng.*, 122(3), 173–180.

Mori, Y., and Ellingwood, B. R. (1994). "Maintaining reliability of concrete structures. II: Optimum inspection / repair." *J. Struct. Eng.*, *10.1061/(ASCE)0733-9445(1994)120:3(846)*, 846–862.

Neal, R. M. (2003). "Slice sampling." *Ann. Stat.*, 31(3), 705–767.

Neves, L. C., Frangopol, D. M., and Cruz, P. J. S. (2006a). "Probabilistic lifetime-oriented multiobjective optimization of bridge maintenance: single maintenance type." *J. Struct. Eng.*, 10.1061/(ASCE)0733-9445(2006)132:6(991), 991–1005.

Neves, L., Frangopol, D., and Petcherdchoo, A. (2006b). "Probabilistic lifetime-oriented multiobjective optimization of bridge maintenance: combination of maintenance types." *J. Struct. Eng.*, 10.1061/(ASCE)0733-9445(2006)132:11(1821), 1821–1834.

Onoufriou, T., and Frangopol, D. M. (2002). "Reliability-based inspection optimization of complex structures: a brief retrospective." *Comput. Struct.*, 80(12), 1133–1144.

Orcesi, A., and Frangopol, D. M. (2011). "Use of lifetime functions in the optimization of nondestructive inspection strategies for bridges." *J. Struct. Eng.*, 10.1061/(ASCE)ST.1943-541X.0000304, 531–539.

Paris, P. C., and Erdogan, F. A. (1963). "Critical analysis of crack propagation laws." *J. Basic Eng.*, 85(4), 528–534.
Perrin, F., Sudret, B., and Pendola, M. (2007). "Bayesian updating of mechanical models-application in fracture mechanics." *18 ème Congrès Françes de Mèçanique*, Grenoble, France, AFM, Maison de la Mécanique, Courbevoie, France, 27–31.
Soliman, M., Frangopol, D. M., and Kim, S. (2013). "Probabilistic inspection planning of steel bridges with multiple fatigue sensitive details." *Eng. Struct.*, 49, 996–1006.
Zheng, R., and Ellingwood, B. R. (1998). "Role of non-destructive evaluation in time-dependent reliability analysis." *Struct. Safe.*, 20(4), 325–339.